

# **Army Research Laboratory**

Aberdeen Proving Ground, MD 21005-5067

---

---

**ARL-TR-2367**

**November 2000**

---

## **A Computational Model of Soman-Induced Cardiac Toxicity (I): Simulation at the Cellular Level**

**Csaba K. Zoltani**

Corporate Information and Computing Directorate, ARL

**Steven I. Baskin**

U.S. Army Medical Research Institute of Chemical Defense

---

## **Abstract**

---

Under a memorandum of understanding (MOU) between the Computational and Information Sciences Directorate (formerly the Corporate Information and Computing Directorate) of the U.S. Army Research Laboratory and the U.S. Army Medical Research Institute of Chemical Defense, results of a study to model the electrophysiological changes in the heart due to soman toxicity are reported. This, the first of a series of reports, presents a computational model of cardiac toxicity at the cellular level and shows the changes in electrical activity for a series of organophosphate (OP) dose concentrations expressed by changes in the acetylcholine concentration generated membrane currents. A plausibility argument is advanced for the consideration of an overlooked aspect of the problem, the effect of extracellular potassium ion accumulation, to the understanding of soman-induced electrophysiological chaos.

## Acknowledgments

It is a pleasure to thank D. Maxwell and R. Sweeney for pointers on soman experimental data and Dr. M. Adler of USAMRICD for his comments. Special thanks go the U.S. Army Research Laboratory (ARL) and the USAMRICD library staffs who went the extra mile to obtain information requested.

INTENTIONALLY LEFT BLANK.

# Table of Contents

	<u>Page</u>
<b>Acknowledgments</b> .....	iii
<b>List of Figures</b> .....	vii
<b>List of Tables</b> .....	ix
<b>1. Introduction</b> .....	1
<b>2. Methods and Materials</b> .....	4
2.1 Prior Work .....	4
2.2 The Electrophysiological Model .....	7
2.3 ACh Accumulation: The Purves Model .....	13
<b>3. Computational Approach</b> .....	16
<b>4. Results</b> .....	17
<b>5. Discussion</b> .....	22
5.1 Effect on the SA Node .....	22
5.2 Effect on the Purkinje Fiber .....	24
5.3 Effect on the Ventricle .....	24
5.4 Effect of Extracellular Potassium Concentration .....	24
5.5 Summary .....	26
<b>6. References</b> .....	29
<b>Appendix</b> .....	33
<b>Glossary</b> .....	41
<b>Distribution List</b> .....	43
<b>Report Documentation Page</b> .....	45

INTENTIONALLY LEFT BLANK.

## List of Figures

<u>Figure</u>		<u>Page</u>
1.	Schematic of ACh Discharge From Nerve Endings, After Feldman et al. (2000).....	3
2.	Electrical Pathways of the Heart.....	7
3.	Schematic of the Synaptic Process After Hille (1992).....	8
4.	Schematic of the More Important Membrane Current Pathways of a Cell.....	10
5.	Second-Messenger Pathways in the Cardiac Cell Membrane, After Hille (1992).....	11
6.	Action Potential of the Rabbit SA Node Under Normal Conditions.....	18
7.	Action Potential of a Sinoatrial Cell.....	19
8.	Top Curve Shows the Action Potential in the Purkinje Fiber Cell.....	19
9.	Effect of ACh-Activated Potassium Current on a Ventricular Cell.....	20
10.	Effect of the Change in the Concentration of $[K^+]_o$ on the AP of the SA Node.....	21
11.	Effect of the Change in the Concentration of $[K^+]_o$ on the AP of the Purkinje Fiber.....	21

INTENTIONALLY LEFT BLANK.

## List of Tables

<u>Table</u>		<u>Page</u>
1.	Summary of Effect of ACh on Cardiac Function.....	2
2.	Simulation Studies of the Effect of ACh Concentration on Membrane Currents.....	14
3.	Contrast of Cell Behavior With Increase in ACh-Induced Potassium Current.....	22
A-1.	Rate Constants and Concentrations Used in the Simulation.....	40

INTENTIONALLY LEFT BLANK.

# 1. Introduction

Pulmonary and cardiac symptoms are the primary indicators of soman poisoning. The cardiac effects are discussed in detail in this report. The primary interests are the underlying electrophysiological changes at the cellular level that manifest themselves in bradycardia, arrhythmia, and asystole.

Soman belongs to the class of organophosphate (OP) nerve agents that are also used in the civilian sector in insecticides. OP can induce a wide variety of toxic physiological changes, as discussed for example by Roth et al. (1993), Hassler et al. (1988), and Golomb (1999). OP binds to acetylcholinesterases (AChE) (Hartzell 1988), preventing hydrolysis and leading to an increase in acetylcholine (ACh). This overload changes the activity of the sinoatrial (SA) node and causes negative inotropy and arrhythmia not only in the atria (bradyarrhythmia), but also in the Purkinje fibers; it also produces electrical conduction anomalies. In addition, the absence of cholinergic agonists increases the calcium influx and stimulates its uptake in the sarcoplasmic reticulum (SR), thereby increasing the intracellular calcium. There is some evidence (Wang 1997) that an overload of cellular  $Ca^{++}$  within the SR can also lead to atrial arrhythmias.

ACh dramatically alters gating properties of cellular membrane channels, such as  $i_{K1}$  channels. It increases intracellular  $Na^+$  activity. The physiologic changes are not uniform in all cardiac structures. The Purkinje fibers and the SA node experience different degrees of impairments than the ventricles and atria. Other factors may also enter the picture. A rise in plasma acetylcholine is accompanied by a fall in coronary blood flow. According to McKenzie (1996), OP toxicity is thought to lead to "vasospasm followed by myocardial ischemia and cardiac dysfunction." The cardiac muscle is mainly aerobic. An excess of acetylcholine at muscarinic myocardial receptors sites results in an increase in oxygen uptake in the muscle. Blocking these muscarinic sites with atropine can lead to myocardial infarction in hypoxemia.

High concentrations of ACh also elicit negative inotropic effects. Ancillary manifestations are lesions in the atrium, hypotension, and vasodilatation. In rats, soman-produced ECG changes

include reduced P-wave height, prolonged P-Q interval, a QRS complex, and AV-block. There is scant in vivo data in man, but cholinesterase inhibition is known to cause increased electric systole and, in some cases, torsade de pointes (Baskin and Whitmer 1991).

At the cellular level, ACh increases  $K^+$  permeability (conductance) via G-protein-gated channels leading to

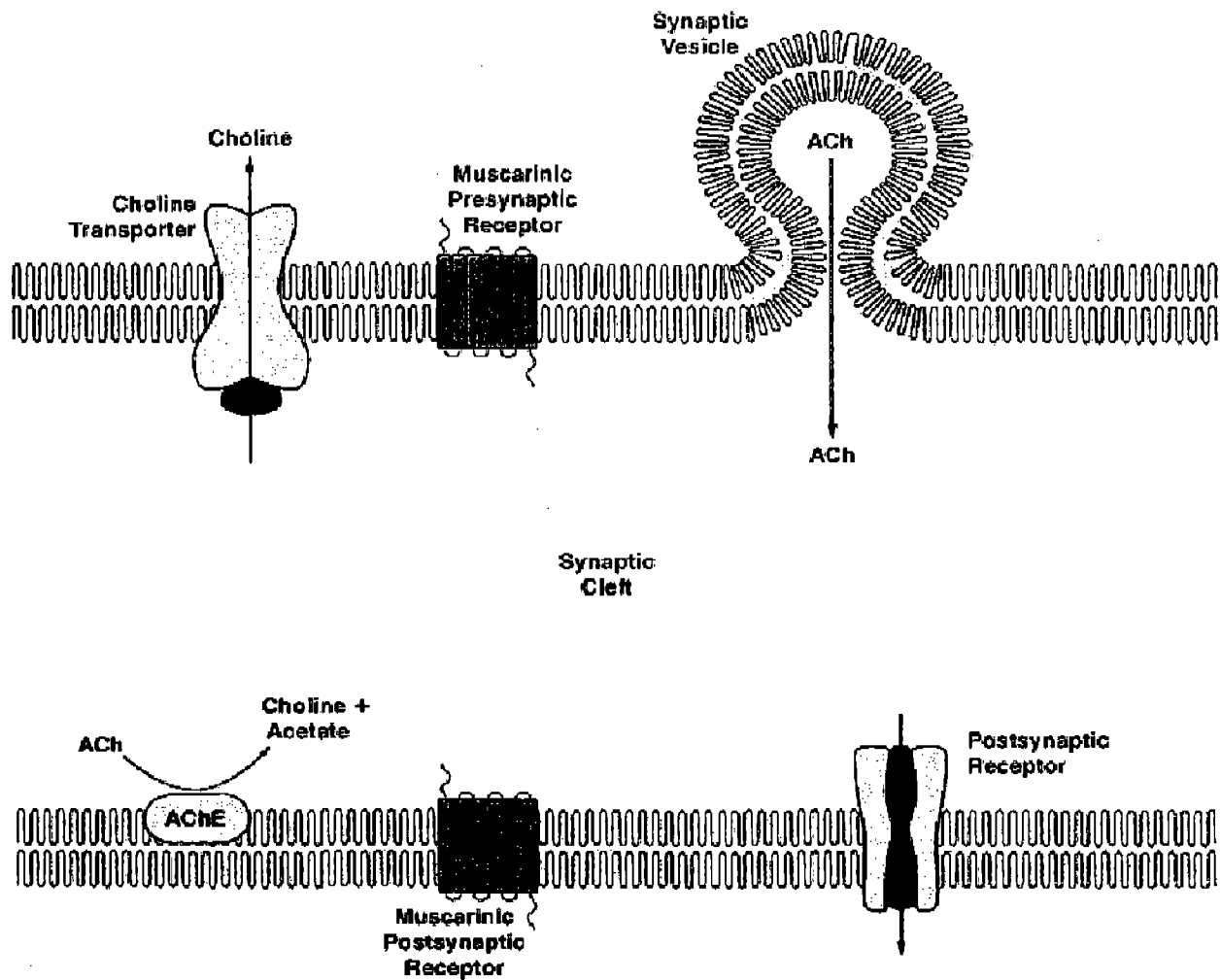
- (1) opening activation gates of  $i_{K,ACh}$ ,
- (2) decreasing amplitude and duration of action potential, and
- (3) slower pacemaker depolarization.

Table 1 shows the effect of ACh on cardiac function. OP agents antagonize (AChE) at cardiac sites, leading to an excess of ACh and atrial modulation of the negative chronotropic effect of ACh. The basic assumption is that since AChE is vital to survival, once its concentration falls below a certain limit, which varies among animal species, the subject dies. Green (1958) suggests that  $LD_{50}$  be defined as 10% of the essential level needed for survival in the absence of an acetylcholine antagonist.

**Table 1. Summary of Effect of ACh on Cardiac Function**

SA Node	Decreases rate of spontaneous diastolic depolarization. Hyperpolarizes node.
AV Node	Slows conduction. Lengthens refractory period.
Atrium	Shortens AP and refractory period duration.
Purkinje Fibers	May shut be shut down by excess.
Ventricle	Induces inotropic effect.

There is a parallel between soman and flouxetine (Prozac group of antidepressants), or for that matter cocaine. Prozac boosts serotonin by blocking reuptake of the neurotransmitter into the cells that originally released it. This leads to elevated levels of serotonin and other neurotransmitters, such as dopamine, while soman acts as an "ACh uptake inhibitor." Figure 1 provides a schematic of ACh discharge from nerve endings modeled after Feldman et al. (2000).



**Figure 1. Schematic of ACh Discharge From Nerve Endings, After Feldman et al. (2000).**

In the present project, a mathematical model of cardiac toxicity induced by OP is under development. Given an LD<sub>50</sub> dose of soman and the ancillary overload of ACh, the question addressed is: What are the effects on the electrophysiology of the heart?

Since cardiac toxicity finds a marked expression in the rabbit, it was adopted as the animal model (Dokos et al. 1998). Where available, references to experiments with other animals are also made. The manifestations of the presence of OP is an ACh overload. In recognizing this, single-cell calculations of the effect of ACh overloading are presented using the Oxford Heart

program, Oxsoft Ltd. (1997). Particularly, calculations are presented showing how ACh overload affects the individual membrane currents and its overall effect on the resulting action potential. The approach is to gauge the effect of changes in potassium conductance ( $g_K$ ) and two of the membrane currents important in pacemaking ( $i_f$  and  $i_{K,ACh}$ ) on the electrophysiology of the cardiac cell (i.e., the development of the action potential).

It is known that  $[K^+]_o$ , the extracellular potassium concentration, influences the transmembrane resistance in Purkinje fibers. Elevated concentrations result in higher-than-normal conductance. Hyperkalemia can also result in sudden cardiac death. There is a direct causality between soman poisoning and changes in action potential (AP) of the heart, and the connection is investigated in this report. This investigation leads us to suggest the importance of the overlooked aspect of soman intoxication, excessive potassium extracellular concentration, and propose possible new avenues for therapy.

The answers to several subsidiary and important questions are deferred for later. These include the effect of the toxic environment-induced gene mutation of ion channel configuration, the effect of the "aging" process affecting AChE-OP complex, and the presence of OP scavengers on the ionic currents.

## 2. Methods and Materials

**2.1 Prior Work.** Baskin et al. (1991) summarized much that was known about cardiac toxicology due to OP agents. Subsequently, experimental observations of the effect of soman in general have appeared, but little related specifically to the heart. Computational models remain scarce; with few exceptions, those existing address ancillary issues such as the effect of ACh pulses on the membrane ion dynamics.

The effect of ACh on individual sinoatrial node cells includes activating the acetylcholine-activated potassium current,  $i_{K,ACh}$ , which indirectly decreases the L-type calcium current and the hyperpolarization-activated current,  $i_f$ . Using this formalism, Sears et al. (1999)

studied postexercise heart rate mimicked by higher potassium concentration and its effect on  $i_f$  and  $i_{K,ACh}$ .

Several research groups have presented mathematical models of the effect of repeated pulses of ACh on the action potential on pacemaker cells. Yanagihara et al. (1980) showed that for the rabbit SA node, an ACh-induced K current ( $i_{K,ACh}$ ) with ACh concentrations of  $5 \times 10^{-8}$  and  $10^{-7}$  decreased the spontaneous frequency from 173 to 132 and 79 beats/min, respectively. At a concentration of  $2 \times 10^{-7}$ , it ceased completely. They noted that the hyperpolarization was caused by a gradual activation of  $i_{ACh}$ , with a time constant of 110 ms.

Michaels et al. (1984) showed the phase dependence of a brief (50 ms) ACh pulse on the action potential. A pulse introduced at 127 ms produced a hyperpolarization of 4.9 mV, and the cycle was lengthened by 112 ms. The same pulse applied later at 280 ms hyperpolarized the membrane by 17.5 mV and prolonged the cycle to 548 ms. This was in line with earlier experimental findings that introducing the pulse later produces longer cycle times. Higher concentrations of ACh elicit larger phase shifts. It was also noted that at very late times in the cycle, a "latent" period is observed (i.e., the ACh pulse effects are postponed until the following cycle). Repetitive acetylcholine input synchronization of the sinus pacemaker was observed.

Dexter et al. (1989a, 1989b, 1994) developed a mathematical model to predict the rate of degradation of ACh in the neuroeffector junction. A decline of the sinus period in anesthetized dogs was observed.

Dokos et al. (1996) presented a single-cell model of the chronotropic response of the SA node to brief-burst vagal stimulation by acetylcholine. The three submodels discussed were the ACh release by vagal stimulation at the SA node and activating  $i_{K,ACh}$  when ACh binds to muscarinic receptors. These rely on data taken from guinea pig myocytes. The second submodel is a three-compartment model of ACh kinetics at the neuroeffector junction. Finally, ACh-inhibited  $i_f$ , operative only in cardiac tissue capable of spontaneous activity, and  $i_{Ca,L}$  in SA cells are discussed. Data taken on rabbit SA node cells were used. The effect of ACh was

shown by Dokos to result in strong hyperpolarization of the membrane and a prolonged cycle in a phase-dependent manner. In a related paper, Dokos et al. (1997) showed for a cycle length recovery after prolonged vagal stimulation for a single-cell rabbit SA node. Refer to Table 1 for a summary or see Dokos et al. (1998) and Demir et al. (1994).

These models rely on the Hodgkin-Huxley (HH) formalism whereby the experimental ionic current data is curve-fitted and coupled to first-order activation equations of the form

$$du/dt = \alpha_u * (1 - u) - \beta_u * u, \quad (1)$$

where  $u$  is a gating variable, and the coefficients of opening and closing,  $\alpha_u$  and  $\beta_u$ , are functions of the ACh concentration. Dokos et al. (1997) has subsumed the effect of the G-protein into this formulation.

Other related works are those of Trautwein and Dudel (1958), Magleby and Stevens (1972), Bristow and Clark (1983), and Egan and Noble (1987). Ancillary chemical effects of ACh inhibition of the SA node were examined by Kale et al. (1999). They were able to demonstrate the suppression of cAMP by acetylcholine by G-protein effects.

Sweeney and Maxwell (1999) presented a single compartment model of an OP interaction with AChE and CaE, OP scavengers. They obtained an "OP toxicity surface" that shows, for example, relative initial concentrations of OP/AChE as a function of the binding rate of CaE/AChE, where hydrolysis and CaE protect against OP poisoning (see also Maxwell et al. 1988, 1991).

Though useful contributions to the general understanding, none of these authors offer a comprehensive and quantitative approach to the changes induced in the cellular dynamics and the resulting pathologies caused by soman. This report contributes to establishing that quantitative relationship.

**2.2 The Electrophysiological Model.** The SA node may be considered the most important component of the heart due to the centrality of its function. This node consists of a group of specialized cells at the superior portion of the junction between the right atrium and the superior vena cava, and it controls the rhythm of the heart, see Figure 2. In turn, the behavior of its constitutive cells depends on the synchronous functioning of at least eight membrane currents. Thus, examining the vulnerability of these cells to OP toxicity is a logical starting point in these studies.

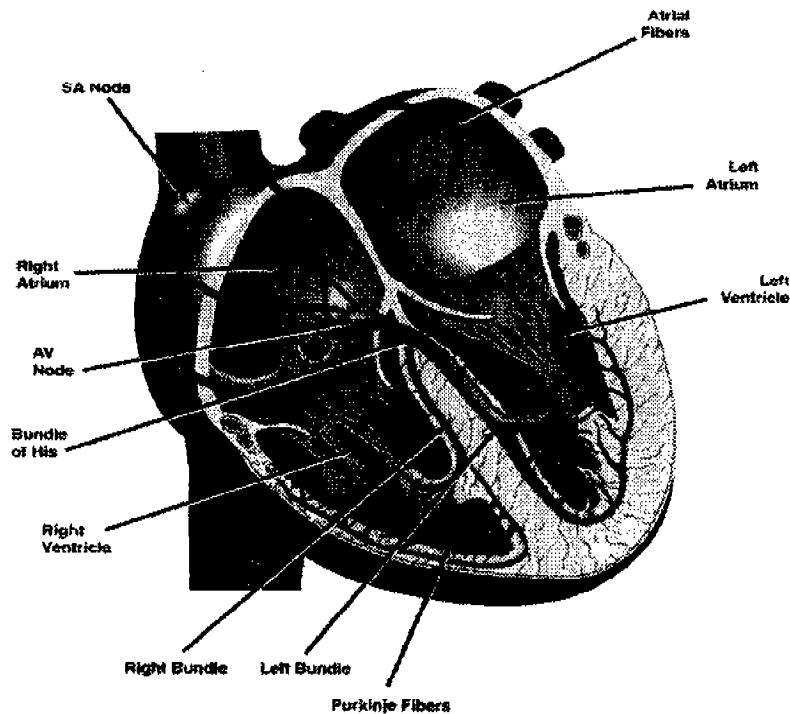


**Figure 2. Electrical Pathways of the Heart.**

The parasympathetic innervation of the cardiovascular system occurs through the vagus nerve. The innervation is thought to be limited to the SA node and the atrioventricular (AV) junction. The ventricles participate little, if at all, in this process, although ACh binds to the receptors in the endothelium, the layer of cells that line the heart. ACh binds to the muscarinic receptors of the target tissues (i.e., the SA node), the AV junction, and the endothelium.

Nerve impulses into the axon terminal trigger the processes that lead to release of ACh, followed by interaction with the acetylcholine receptors, and conductance increase of specific ion channels in the postsynaptic membrane (Rosenberry 1979) and postsynaptic endplate currents, see Figure 3. These sequence of events then contribute to the processes that result in the action potential and, ultimately, the expansion and contraction of the heart muscle.

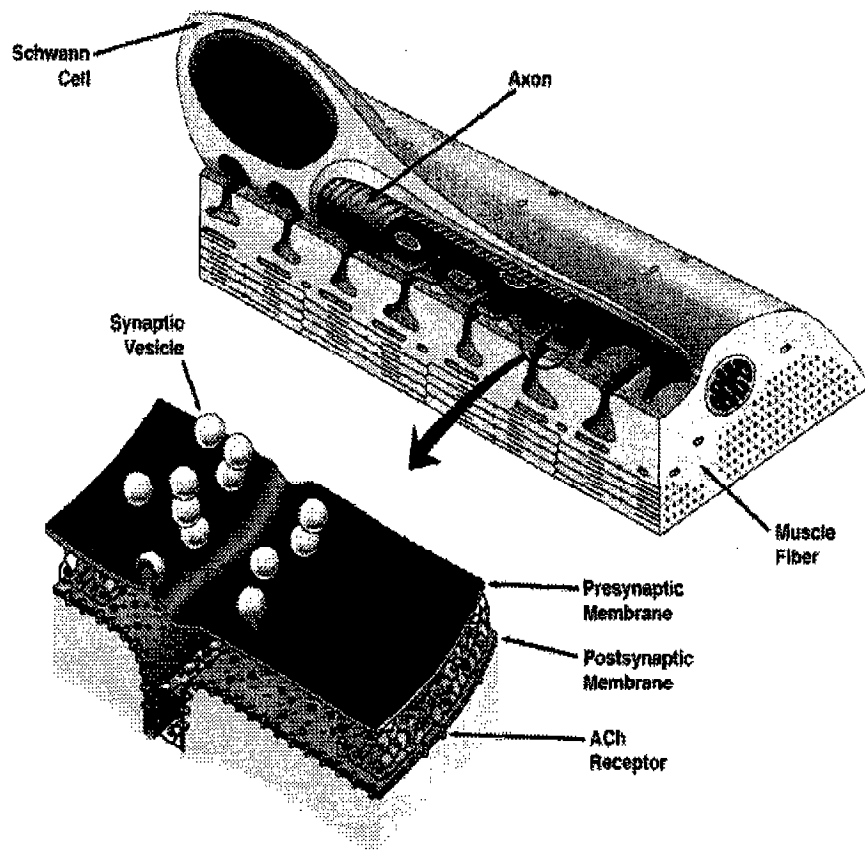


**Figure 3. Schematic of the Synaptic Process After Hille (1992).**

Katz (1992) defines pacemaker activity as “an instability of diastolic (resting) potential that initiates a propagated action potential.” The pacemaker activity is the result of the decay of the delayed, outward rectifier current ( $i_K$ ) that appears during the plateau of the action potential. The inward, anomalous rectifier current ( $i_{K1}$ ) also contributes to the pacemaker activity.

There are two primary inward currents ( $i_{Ca}$ ) active at the end of repolarization; they regulate cardiac contraction and  $i_f$ , the most important pacemaker current. The sodium current mediates

the heart rate by the autonomic nervous system. This is apparent from the changes in the slope of the diastolic depolarization.

Heart rate is slowed by vagal stimulation and increased by  $\beta$ -adrogenic agonists. In turn, these are mediated by  $G_i$  and  $G_o$  proteins on channels that carry  $i_f$ .  $G_i$  is inhibitory and dominating and causes vagal slowing.

Both the Na and the K conductance change during depolarization. While Na permeability rises rapidly before decaying, K conductance attains a plateau and subsequently decreases rapidly to resting levels during repolarization.

One of the earliest works on  $i_{K,ACh}$  was by Osterrieder et al. (1980, 1981). Of the five muscarinic receptors, he noted that the  $M_2$  and  $M_4$  receptors inhibit adenylate cyclase (ADC) activity. These receptors preferentially couple the  $G_{i/o}$  family of G proteins. Inhibiting ADC reduces the phosphorylation of the L-type  $Ca^{++}$  channel, reducing  $i_{Ca,L}$ , and reducing the hyperpolarization activated current  $i_f$ . Cholinergic inhibition of  $i_{Ca,L}$  was also observed (Demir et al. 1999) due to cGMP-stimulated cAMP. Phosphodiesterase (PDE) hydrolyzes cAMP, thus inhibiting cAMP-dependent phosphorylation of L-type  $Ca^{++}$  channels, see Figure 4.

In muscarinic ACh-dependent channels, activating  $i_{K,ACh}$  requires splitting a CTP-binding G-protein. When both  $G_i$  and  $G_o$  are antagonized,  $i_{K,ACh}$  is eliminated.

The direct effect of ACh is expressed by activating the ACh-sensitive  $K^+$  channel. Binding a muscarinic agonist to a receptor results in a configuration change, and a signal is sent to the G-protein in the membrane lipid bilayer. GTP binds to an  $\alpha$ -subunit and activates the G-protein. In the process, the G-protein dissociates into the  $\alpha$ ,  $\beta\gamma$  subunits, which enable the channel opening. The deactivation results upon the hydrolysis of GTP to GDP, and the channel closes as a result.

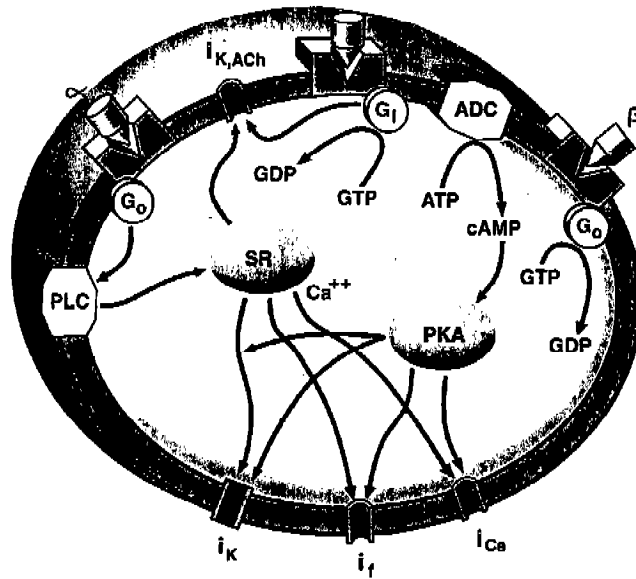


**Figure 4. Schematic of the More Important Membrane Current Pathways of a Cell.**

The indirect action of ACh is expressed when ACh binds to muscarinic receptors and activates the  $G_i$  protein, resulting in the inhibition of the activation of ADC. This step slows the activation of cAMP-dependent protein kinase and reduces the phosphorylation of  $Ca^{++}$  channels.

There are two paths, direct and indirect. In the direct pathway, the neurotransmitter ACh activates the GTP-ase of the  $G_i$  protein.  $\beta\gamma$  subunits bind to the  $K_{ACh}$  channel, causing an increase in the muscarinic current  $i_{ACh}$ . See Figure 5 and Accili et al. (1998).

The intracellular second messenger, cAMP, mediates the indirect effect. Changes in cAMP produce  $i_f$ . In summary then, the SA node pacemaking potential results from

- (1) the decay of the outward flowing  $K^+$  current  $i_K$ , which was activated during the previous action potential cycle (the decay mediates inward background current to depolarize the cell);
- (2)  $i_f$ 's contribution to the depolarization becoming prominent as the diastolic potential becomes more negative;

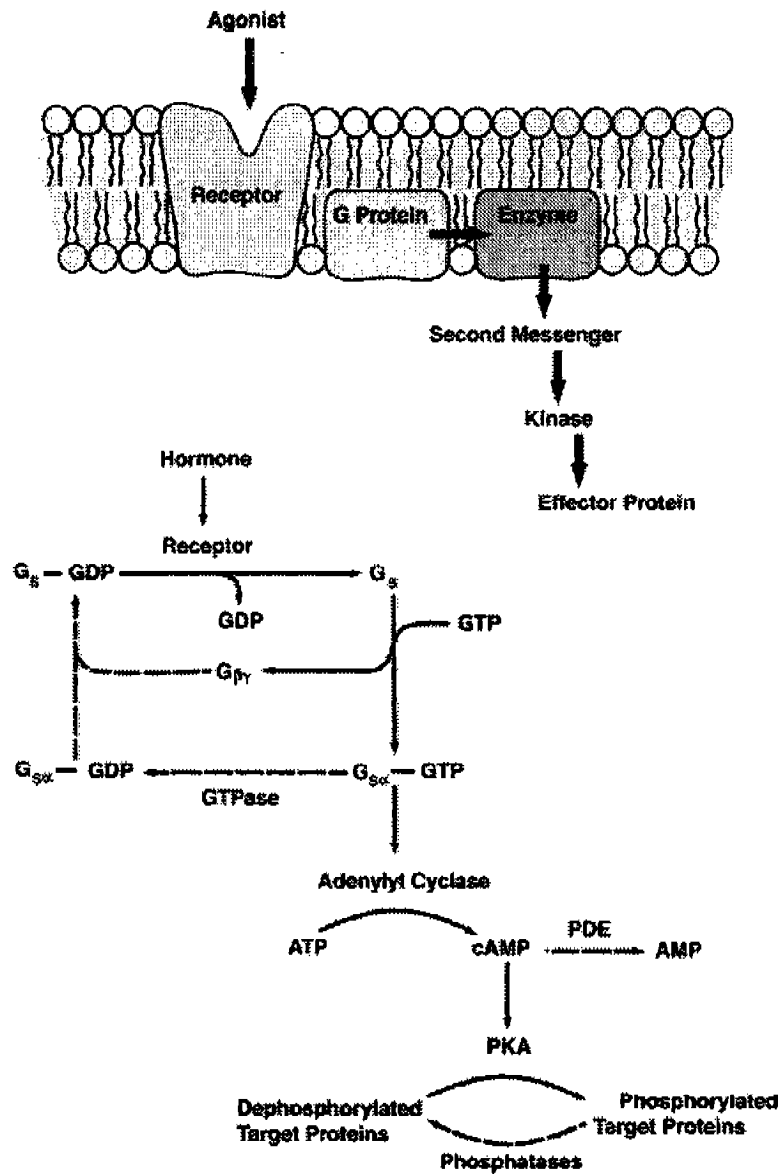


**Figure 5. Second-Messenger Pathways in the Cardiac Cell Membrane, After Hille (1992).**

- (3) the  $i_{Ca}$  current becoming important in the later portion of the cycle; and
- (4) the possibility of the Na-K pump currents and Na-Ca exchanger currents playing secondary roles.

During prolonged exposure to ACh, the level of  $i_{K,ACh}$  fades from desensitization. This current is thought to be directly activated by the G-protein  $G_K$  that links the muscarinic receptor to  $K^+$  channel; thus, it has been postulated that desensitization is a result of modifying the  $G_K$  protein or the  $K^+$  channel. Zang et al. (1993) reported a reduction to 22% of the peak value over time of the current when muscarinic receptors are activated by ACh (see also Boyett et al. 1995).

In this, the first of a series of communications, the changes in the electrophysiology of a single cell of the SA node, Purkinje fiber, and ventricle are considered. The effect of an overload of ACh is examined, as expressed by the membrane currents, which are in turn responsible for the action potential in these cells. The initial calculations consider only ACh overload based on soman  $LD_{50}$  data for rabbits.

Cell models continue to evolve. For the SA node, the models of Demir et al. (1994, 1999) are the most up to date. Until 1985, the Purkinje fiber cell models did not treat the pacemaking currents correctly. The DiFrancesco-Noble formulation, which comes in several forms, is now accepted as the closest to experimental observations. For ventricular cells, the Noble et al. (1991) model and its improvements are most widely used.

When the vagal nerve is continuously stimulated or ACh is applied to a tissue sample, ACh has a negative chronotropic, inotropic (influencing contractility), and dromotropic effect (factors that change the time needed to complete one beat). Due to phosphorylation or dephosphorylation, these fade over time as a result of desensitization. On the other hand,  $i_f$  and  $i_{ca}$  are unaffected. In particular, note the following:

- (1) A low dose of ACh inhibits  $i_f$  by the indirect pathway. The  $i_f$  activation curve is shifted in the hyperpolarization direction.
- (2) High doses of ACh ( $10^{-6} - 10^{-3}M$ ) activate the muscarinic  $K^+$  current  $i_{K,ACh}$  by the indirect pathway.

- (3) ACh produces conductance change, whereby the  $K^+$  ionic channels are enabled.
- (4) ACh affects  $i_f$  at concentrations lower than that required to affect  $i_{K,ACh}$ .
- (5) The effect of ACh on  $i_{K,ACh}$  shows rapid desensitization.
- (6) ACh inhibits the L-type calcium current,  $i_{Ca,L}$ .

Table 2 summarizes the simulation studies that included the effect of ACh on membrane currents.

**2.3 ACh Accumulation: The Purves Model.** The amount of ACh present in the synaptic cleft is one of the crucial variables in the problem. The hypothesis undergirding this study is that the persistence of an excess of ACh is a direct measure of the effect of soman on the heart. Thus, it is important to establish the expected concentration of ACh for a given soman loading.

ACh is stored in a large number of vesicles in the presynaptic endplate terminal whose area is taken to be typically to be around  $2,000 \mu m^2$ , and the density of receptors on the average is around  $2 \times 10^7$  (Michelson and Zeimal 1973; Katz 1969; Koelle 1963). Assuming the number of AChE molecules near the neural effector junction to be of the same order as the number of receptor sites, the presence of  $10^7$  soman molecules would deprive all sites of AChE and thus from hydrolyzing ACh. It follows that a concentration of soman of the same order or greater would mediate the maximum effect in  $i_{K,ACh}$  and  $i_f$ .

Purves (1977) showed that the ACh concentration after a single stimulus to the vagus nerve can be expressed as

$$[ACh](t) = \frac{MU(t-t_0)}{[\pi D(t-t_0)]^{1.5}} \exp\left[-k_h(t-t_0) + \frac{x^2}{4D(t-t_0)}\right], \quad (2)$$

**Table 2. Simulation Studies of the Effect of ACh Concentration on Membrane Currents**

Reference	Animal Model	ACh Concentration	Pulse Width	Effect(s) Noted	Tools Used
Yanagihara et al. (1980)	Rabbit SA	$5 \times 10^{-8}$ M $1 \times 10^{-7}$ M $2 \times 10^{-7}$ M	—	Heart Frequency	ACh Concentration
Bristow and Clark (1983)	Rabbit SA	—	—	Cycle Length	Bursts of ACh
Michaels et al. (1984)	Rabbit SA	$1 \times 10^{-6}$ M	50 ms	Cycle Length	Single, Repetitive ACh Pulses
Noble and Noble (1984)	Mammalian SA	—	—	Frequency	$K_o$ Concentration Change
Egan and Noble (1987)	Rabbit SA	$1 \times 10^{-4}$ M, $2 \times 10^{-6}$ M	—	Cycle Length Arrest Condition	K-current Conductance Change ACh Conductance Change
Dexter et al. (1989a)	—	50 nM	—	Half Life	Vagal Stimulus
Dokos et al. (1993)	Rabbit SA	0.001 mM to 0.01 mM	—	Cycle Length	ACh Pulse
Zhang et al. (1999)	Rabbit SA	0.09mM and 0.1 mM	—	Shift	ACh Concentration
Sears et al. (1999)	Guinea Pig	$i_{K,AC}$ set at 50 pA	—	Frequency	Extracellular K at 3, 4, 8, 10 mM
Demir et al. (1999)	Rabbit SA	0, 10, 100 nM	—	Frequency	Bath, Vagal Stimulus

where  $U = 1$  for  $t > t_0$ , and

$$U(t - t_0) = 0 \text{ elsewhere.} \quad (3)$$

Here,  $t_0$  is the time of the quantal release, and  $M$  is the amount of ACh. The total ACh is the sum over all the bursts. The equation takes both diffusion and chemical change into account.

There,  $x$  is the distance between release sites, typically  $7.5 \times 10^{-6}$  cm, and  $D$  is the diffusion constant. Bristow and Clark (1983) give a value of  $5.14 \times 10^{-11}$  cm<sup>2</sup>/s for the diffusion constant. They found an ACh concentration per pulse of 0.1  $\mu$ M. This is considerably higher than the  $10^{-17}$  moles per nerve impulse (or  $5 \times 10^6$  molecules of ACh liberated) cited by Michelson and Zeimal (1973). The latter authors also state that between 200 and 300 vesicles are discharged in the synaptic cleft in 1 ms.

The hydrolysis rate constant,  $k_h$ , has a value of  $50 \text{ s}^{-1}$ . Enzymatic hydrolysis of ACh terminates the action. Also, frequent stimulation results in exhausting the ACh stores in the nerve endings.

In the effective stimulus,  $S$  in a plane, where the receptors cover a plane of radius  $r$ , with  $r$  very large

$$S = \frac{BM}{(\pi Dt)^{0.5}} \exp(-x^2/4Dt), \quad (4)$$

where  $B$  is a constant and, as stated by Purves (1977), "relates to the sensitivity, etc., of the receptors and whose dimensionality is appropriate to the particular circumstances."  $M$ , as before, is the amount of released ACh.

Maxwell et al. (1991) noted that, for the rabbit SA node,  $EC_{50}$ , for contraction in the atria, the concentration necessary to produce 50% of the maximum response was  $4.1 \times 10^{-6}$  M for ACh.

At the same time, they reported that soman concentration of  $10^{-6}$  M or greater produced complete ACh inhibition. Thus, for the rabbit SA node, it is not unreasonable to hypothesize that ACh concentrations exceeding  $EC_{50}$  are of special interest and would mediate the maximum effect in  $i_{K,ACh}$  and  $i_f$ .

### 3. Computational Approach

The computational model is based on the electrical representation of the cardiac cell by a system of equations expressing the electrical and chemical activity of the cell.

The presence of OP was simulated by an increased presence of ACh, as reflected in  $i_{K,ACh}$ ,  $i_f$ , and a change in the potassium conductance. In addition, simulations were run with varied extracellular potassium concentrations. The rate of change of the membrane voltage, equation (A-26) was solved, with the membrane currents depending on a model such as equations (A-1)–(A-32).

A Runge-Kutta-Merson integration with automatic step-size adjustment based on error size was used to solve the system of equations. Single cell calculations were run on an NT workstation. Simulations encompassing large arrays of cells, in preparation at the present time, require the 128-node Origin 2000 of the MSRC.

In the first series of calculations of a SA-node cell, the potassium current induced by ACh was increased from the normal condition up to where soman was thought to have neutralized in excess of 95% of the AChE.

The calculations were repeated, but with the external (to the cell) potassium concentration changed from the normal state of 5.4 mM to 10.0 mM. The ACh overload calculations were also repeated for the Purkinje fiber and the ventricular cells.

## 4. Results

This computational study was directed at examining how membrane currents change in response to concentration changes in ACh induced by the presence of soman. This allows for determining the critical conditions that culminate in the shutdown of the action potential. The sensitivity of the SA-node, the Purkinje fibers, and the ventricular cells could then be contrasted and compared with experimental data from the literature. Oxsoft Heart, version 4.8 (Oxsoft Ltd. 1997), was used in the calculations.

The result of the set of runs is shown in Figures 6–11. Changes in concentration of ACh were expressed in the induced currents and approximated the effect of a soman level corresponding to LD<sub>50</sub>.

The important observations of this study are the following.

- (1) An ACh overload can suppress the action potential of the Purkinje fibers.
- (2) In line with and in addition to earlier experiments and published data, ACh overload not only produces bradycardia, but can also arrest the heart at high levels of induced K<sup>+</sup> current.
- (3) In the animal model used in this study, the action potential in the sinoatrial node terminated whenever  $i_{ACh,K}$  exceeded 0.0023 nA.
- (4) In the presence of elevated ACh,  $i_f$  is depressed.
- (5) In the presence of ACh,  $i_{Ca,L}$  is depressed.

- (6) ACh overload in the ventricle shortens the action potential notch in the voltage in phase 2, and ultimately ceases the calcium current. This suggests incipient onset of fibrillation.

The action potential of the rabbit sinoatrial cell and calcium membrane current,  $i_{Ca}$ , are shown in the first panel of Figure 6. The resting potential is at  $-50$  mV, and after a gradual rise for  $0.1$  s, there is a steep rise, though much gentler than the corresponding rise in the ventricle. Following the plateau region, the drop steepens as repolarization takes place. Increasing the acetylcholine concentration lengthens the period, as shown in Figure 7, a 20% increase. The action potential ceases at a value of  $i_{K,ACh} = 0.02$  nA.

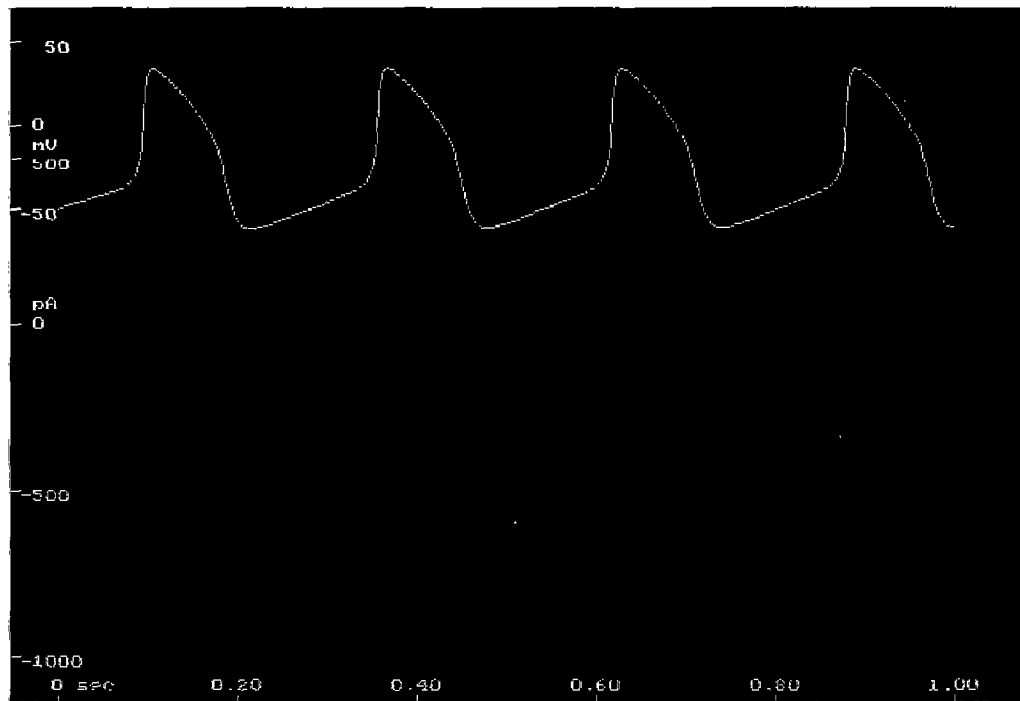


**Figure 6. Action Potential of the Rabbit SA Node Under Normal Conditions. The Top Curve Shows the Action Potential, the Lower Trace  $i_{Ca}$ .**

Figure 8 shows the behavior of the Purkinje fibers to ACh overload induced by  $i_{K,ACh}$ . The action potential is totally suppressed when the current increases to  $9$  nA. Purkinje fibers under ACh overload exhibit bradycardia, and the action potential eventually disappears.

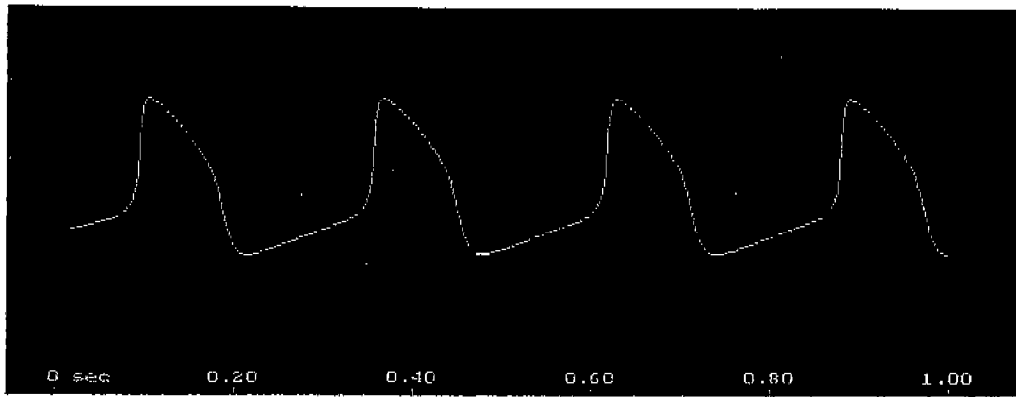


**Figure 7. Action Potential of a Sinoatrial Cell. The Second Displaced Curve Shows the Effect of ACh-Activated Potassium Channel. The Current is 0.0018 nA. When the Current Reaches 0.0024 nA, the Action Potential Ceases, Shown by the Flat Trace.**

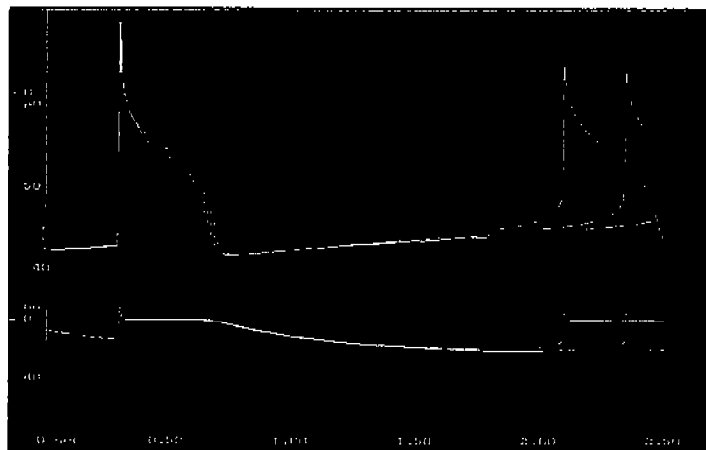


**Figure 8. Top Curve Shows the Action Potential in the Purkinje Fiber Cell. With Increase in the ACh-Activated Potassium Current, the Curve is Shifted, Increasing the Period. The Values of the Activating Current Are 1, 5, and 9 nA, Respectively. At 9 nA, the Action Potential Ceases, Shown by the Flat Trace. The Lower Traces Show the Corresponding  $i_r$  (Grey) and  $i_k$  Currents.**

In Figure 9, the response of a ventricular cell is illustrated. Shutdown occurs at 0.8 nA. The change in  $dv/dt$  in phase 1, at the peak of the curve, is remarkable. The shortening of the period of the action potential, tachycardia, is quite pronounced.

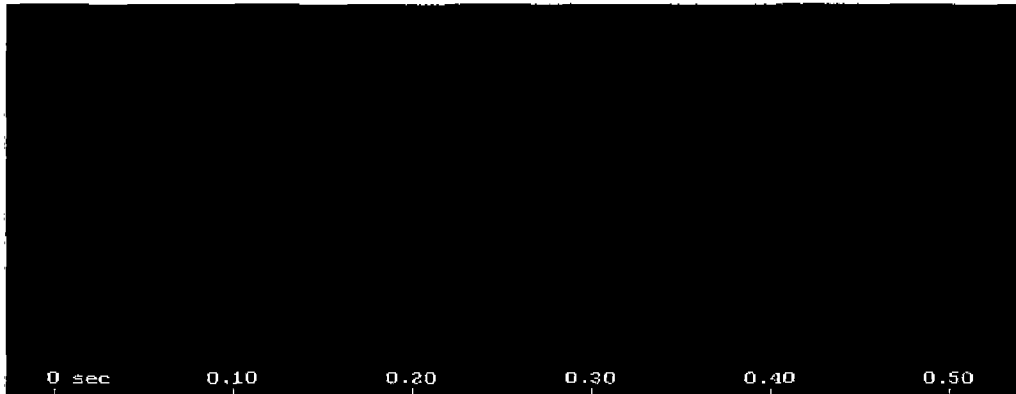


**Figure 9. Effect of ACh-Activated Potassium Current on a Ventricular Cell. As the Current Increases From 0.01 to 0.3, 0.6, and Finally, 0.8 nA, the Period Shortens Continuously, Effectively Extinguishing the Action Potential.**

The magnitude of the calcium current,  $i_{Ca}$ , is also smaller. A notch appears in the action potential curve. With further increase in acetylcholine concentration (not shown), the calcium current practically ceases and the period shortens further.

Figures 10 and 11 show the effect of the extracellular potassium concentration change on the action potential. Note that the magnitudes of the concentrations are considerably different in the two cases. In Figure 10, at a concentration of 30 mM/liter, the action potential is terminated, as shown in flat trace. The green curve represents the calcium current (gray  $i_f$  and violet  $i_K$ ), and  $i_{NaCa}$  is given in blue.

In Figure 11, the flat voltage trace is for  $[K^+]_o = 8$  mM; the right-most and the trace to its left have  $[K^+]_o = 2$  and 4 mM, respectively. The gray trace represents  $i_f$  and the purple  $i_K$ . The negative going  $i_f$  is for  $[K^+]_o = 8$ , and the second largest purple trace is for the starting condition,  $[K^+]_o = 4$  mM/l. Table 3 shows the contrast of cell behavior with an increase in ACh-induced potassium current.

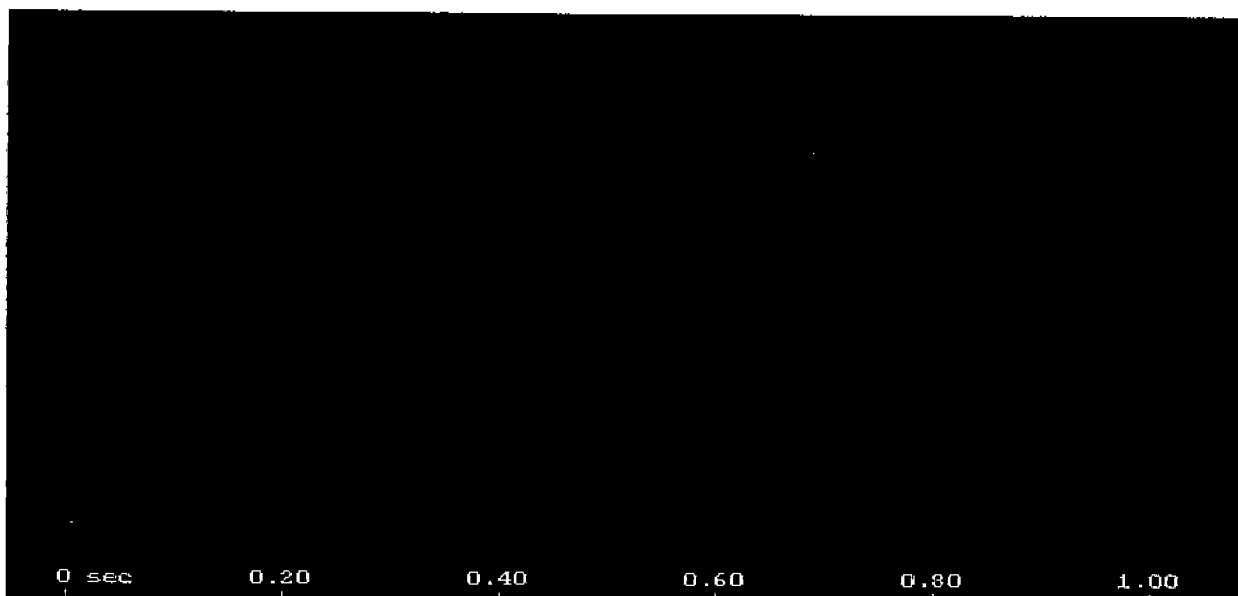


**Figure 10. Effect of the Change in the Concentration of  $[K^+]_o$  on the AP of the SA Node.**

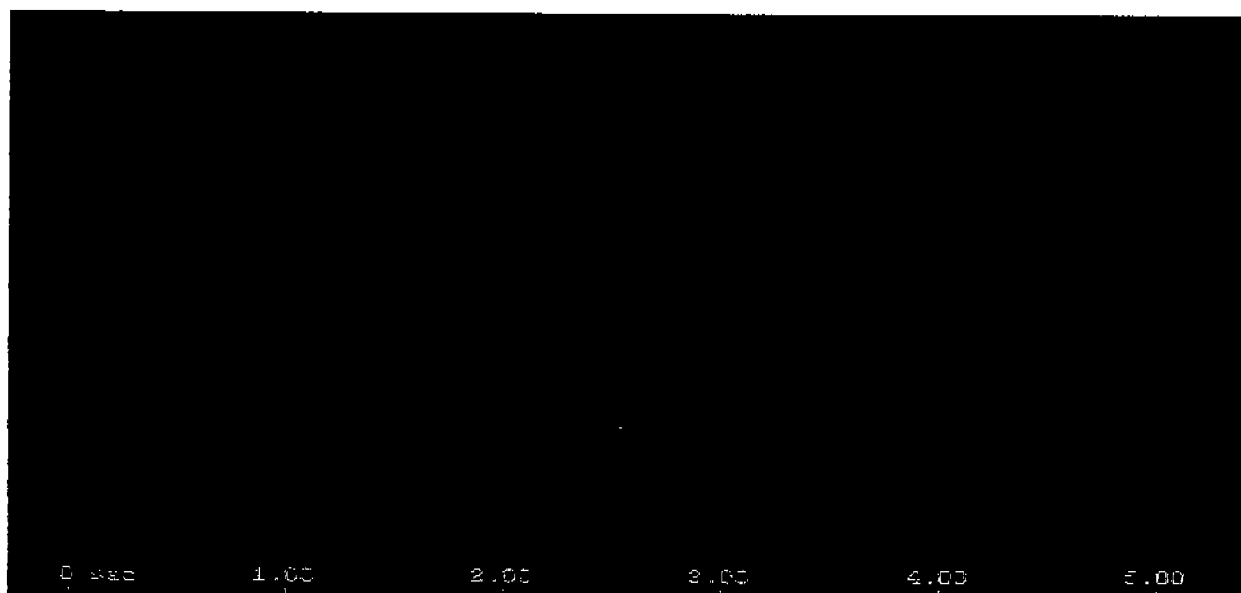


**Figure 11. Effect of the Change in the Concentration of  $[K^+]_o$  on the AP of the Purkinje Fiber.**

**Table 3. Contrast of Cell Behavior With Increase in ACh-Induced Potassium Current**

Cell Type	$i_{K,ACh}$ at Shutdown of Action Potential (nA)	$i_f$ at Shutdown of Action Potential (nA)	AP Duration With Increase in $i_{K,ACh}$
SA Node	0.0024	—	lengthens
Purkinje	9.0	-0.2	lengthens
Ventricle	0.8	—	shortens

## 5. Discussion

Animal studies show that at  $1LD_{50}$  of soman, the accumulated acetylcholine concentration is high enough to arrest the heart. The SA node, the ventricles, and the Purkinje fibers are affected unequally. Evidence points to the SA node cells and the Purkinje fibers as determinants of the outcome.

The primary objective of this study was to elucidate the behavior of the action potential in face of changed membrane currents due to soman-induced ACh concentration change, especially that expressed by  $i_{K,ACh}$  and  $i_f$ . The former current is the best gauge of the effect of acetylcholine overload. In addition, cell environmental changes, such as extracellular  $[K^+]_o$ , were also examined.

**5.1 Effect on the SA Node.** The first series of runs on the SA node cells reported here showed that at a constant high level of ACh, the induced  $K^+$  current,  $i_{K,ACh}$ , lengthens the period of the action potential. With the current at 0.0018 nA, the period is extended by 15%; at 0.0024 nA, the action potential ceases.

A secondary response to ACh is that the inward pacemaker current,  $i_f$ , is inhibited by the G protein. The G-protein inhibits cyclic AMP production, which in turn inhibits the calcium current that plays a role in depolarizing the SA node. One possible outcome is SA block.

These results concur with the findings of Yanagihara et al. (1980) and the data of Osterrieder et al. (1980). They noted that the spontaneous frequency of the heart rate decreased from 173 beats/min to 132 beats/min at an ACh of  $5 \times 10^{-8}$  M, and to 79 beats/min at  $10^{-7}$  M, ceasing completely at  $2 \times 10^{-7}$  M. Zhang et al. (1999), studying the rabbit sinoatrial node with their computer model, found that an ACh concentration of  $7.4 \times 10^{-8}$  M induces a decrease of 50% in the heart rate, and that  $i_{K,ACh}$  is mainly responsible with the shift in  $i_f$  opposing the decrease. Egan and Noble (1987) studied the variations in the SA node activity in response to ACh-activated potassium channels and calcium current permeability. The concentration of ACh, which produced noticeable effect, was  $2 \times 10^{-6}$  M. The maximum potassium current of 0.2–0.3 nA was found at an ACh concentration of  $10^{-4}$  M. Increasing the current to 2 nA lengthened the cycle, while 10 nA arrested the heart. Altering  $i_f$  by increasing the conductance of  $K^+$  and  $Na^+$  from 6–12  $\mu S$  accelerated the heart, while decreasing it to 0 lengthened the cardiac cycle.

The computations were run under the premise that the level of soman in the environment does not noticeably change in the short run. The trends observed from experiments with doses applied for various periods concur with these findings. Bristow and Clark (1983) studied the effect of 1, 2, 3, 5, 7, and 9 pulses per burst of ACh at different times within the cardiac cycle. They showed that when the stimulus is delivered near the peak of the diastolic potential, the cycle length increases to 874 ms from baseline. The channel blocking was simulated by setting  $g_{Na}$  or  $g_{Si}$  to zero. Michaels et al. (1984) induced changes in pacemaker rhythm by single and repetitive applications of ACh pulses. The pulses were simulated by adding ACh-activated potassium current,  $i_{K,ACh}$ , to the membrane equation. An ACh concentration of  $10^{-6}$  M applied at 280 ms of the cardiac cycle shifted the pacemaker cycle duration from 318 to 548 ms.

Considering that the effect of ACh declines over time, the “aging effect” (Dexter et al. 1989a, 1989b) working with dogs found the half-life of ACh after vagal stimulation to be 2.7 s. The sinus period decreased from 550 ms to 410 ms in 15 cardiac cycles after stimulation. The concentration of ACh was 50 nM, and the change in the sinus period depended on the rate of release of ACh.

**5.2 Effect on the Purkinje Fiber.** In contrast to the SA node, considerably larger values of the ACh-induced current, 9 nA, is needed to shut down the action potential. With an increase of the current, there is a gradual shortening of the period starting at baseline. When the current has increased five-fold, the period has lengthened by less than 20%.

This is in line with the experimental work of Carmeliet and Mubagwa (1986). They showed that bath-applied ACh to rabbit Purkinje fibers caused an increase in  $K^+$  conductance, hyperpolarization, and an inhibition of spontaneous activity. In addition, they noted a decrease in  $K^+$  and  $Na^+$  conductance.

**5.3 Effect on the Ventricle.** The ventricle has no pacemaker activity; but still, an ACh overload can arrest its action potential. The cells of the ventricle respond considerably less to changes in ACh concentration than the other two cell types considered, the SA-node cells and the Purkinje fiber cells. The increase in the ACh-activated potassium current has two marked manifestations: shortening the AP period and steepening the slope of the action potential at phase 1, the point of the highest value of the voltage. At a value of 0.8 nA, the AP is not recognizable; it is but a blip of a hundredths of a second duration whose amplitude stays below -50 mV. For all practical purposes, it has been extinguished.

Dokos et al. (1993) also noted that ACh lowers the rate of impulse generation by activating potassium channels, and it also inhibits the hyperpolarized-activated L-type current. An 80-ms ACh pulse of 1- $\mu$ M concentration increased the cardiac period up to 10%; a concentration of 5  $\mu$ M lead to an increase of 35%, while an ACh concentration of 10  $\mu$ M yielded a change of up to 50%. The simulations were made with the modified DiFrancesco-Noble model with  $i_{K_{ACh}}$  included.

**5.4 Effect of Extracellular Potassium Concentration.** Changes in  $K^+$  ion movement are central to expressing soman-induced cardiac toxicity. An ancillary aspect is proposed here that the accumulation of  $K^+$  ions in the interstitial space may play an important role in the overall behavior. The reasoning is as follows: excessive parasympathetic stimulation results in

excessive ACh release. ACh binds to  $M_2$  muscarinic receptors, activates the G-protein, and hyperpolarizes the SA node. When ACh activates  $i_{K_{ACh}}$ ,  $K^+$  exits the cell. The soman-induced ACh overload results in more receptors than usual being bound, also leading to an increase in the external concentration of potassium ions.\*

The two cases shown in Figures 10 and 11 show the effect on the SA node and the Purkinje fibers if the elevated  $K^+$  concentration outside the cell is maintained.

Excessive concentration of  $K^+$  ions changes the concentration gradients and the functioning of the Na-K pump. In the initial stages of the accumulation of the potassium ions, the cells are more excitable, but as the membrane potential drops below the excitation threshold, the generation of an action potential is no longer possible. A two- or three-fold change in the extracellular concentration from the baseline of 4–5 mM can paralyze muscles and arrest the heart. In fact, the rapid loss of potassium ions into the extra cellular fluid can be lethal. It is known that  $[K^+]_o$  below 2 mM and above 9 mM stops the heart. Hyperkalemia suppresses the automaticity of the heart, slows conduction, and leads to bradycardia. It is also characterized by negative inotropy. In man, 98% of the potassium is held intracellularly; thus, a shift of 2% to the extracellular space doubles the concentration of the ion with profound implications.

Indications of hyperkalemia include a flattened P wave on the ECG and, more importantly, in many cases, a tall and narrowed T wave. The literature (see Sidell et al. [1997] for example) does not connect hyperkalemia with soman poisoning, but there is persuasive circumstantial evidence for the case. Some of the changes in the ECG of soman-affected mammals certainly point in that direction. With hyperkalemia in the picture, a number of new antidote strategies suggest themselves.

Though not connected to soman-induced ACh overload, external potassium concentration variation has been studied earlier. Noble and Noble (1984) found that variations in the

---

\* The number of receptor sites available can be very large. Hille (1992) notes that in the frog neuromuscular junction, "there are almost 20,000 binding sites per square micrometer in the top junctional folds of the postsynaptic membrane that lie opposite the active zone of the nerve terminal" (p. 142).

extracellular potassium influenced the frequency of the pacemaker activity. Increasing  $[K^+]_o$  from 2–6 mM lengthened the cardiac cycle. If  $[Na]_i$  was increased from 7.5 mM to 30 mM, the pacemaker activity was stopped. Sears et al. (1999) studied the effect of the changes in the extracellular potassium on the heart-rate frequency. An increase in  $[K^+]_o$  led to a decrease in the heart rate.  $i_{K,ACh}$  was set at 50 pA.

This is in line with the work of Carmeliet and Mubagwa (1986) and, more recently, Cordeiro et al. (1998). They reported that reducing  $[K^+]_o$  from 5.4 mM to 2.0 mM resulted in hyperpolarization of the action potential.

**5.5 Summary.** The computer runs simulated the development of the action potential and the apparent induced physiological abnormalities corresponding to the soman concentration and accompanying ACh overload. While the SA exhibited bradycardia at the same concentration level of ACh, the ventricles exhibit tachycardia. The shape of the action potential of the ventricles also changes, a notch appears at phase 1. With increase in  $[ACh]$ , the notch becomes more pronounced. Also, negative inotropy of the cardiac muscles becomes apparent. All electrophysiological activity was ceased for soman concentrations exceeding  $LD_{50} > 50\%$  in all parts of the heart.

No conclusive evidence was found for or against the postulate that increased  $i_{K,ACh}$  suppresses  $i_f$  (Boyett et al. 1995; DiFrancesco 1994).

The ACh overload effect on the Purkinje fibers, as expressed through the increase in  $i_{K,ACh}$ , is the most critical. When the Purkinje fiber fails, cardiac arrest ensues.

It remains to be determined whether the Zwaardemaker-Libbrecht effect, when rapid changes in  $[K^+]_o$  produce transient arrest of pacemaker fibers, hyperpolarization, and shortened action potential, takes place when large doses of soman are suddenly introduced.

These data suggest that hyperkalemia may play a role in the electrical chaos at the cellular level in soman poisoning. Experiments in the near future should enable a conclusive evaluation of this conjecture.

INTENTIONALLY LEFT BLANK.

## 6. References

- Accili, E. A., G. Redaelli, and D. DiFrancesco. "Two Distinct Pathways of Muscarinic Current Responses in rabbit Sinoatrial Node Myocytes." *Pfluegers Arch. - Eur. J. Physiol.*, vol. 437, pp. 164-167, 1998.
- Baskin, S. I., and M. P. Whitmer. "The Cardiac Toxicology of Organophosphorus Agents." *Cardiac Toxicology*, S. I. Baskin (editor), Boca Raton, FL: CRC Press, 1991.
- Boyett, M. R., I. Kodama, H. Honjo, A. Arai, R. Suzuki, and J. Toyama. "Ionic Basis of the Chronotropic Effect of Acetylcholine on the Rabbit Sinoatrial Node." *Cardiovascular Res.*, vol. 29, pp. 867-878, 1995.
- Bristow, D. C., and J. W. Clark. "A Mathematical Model of the Vagally Driven Primary Pacemaker." *Am. J. Physiol.*, vol. 244 (*Heart Circ. Physiol.*, vol. 13), pp. H150-H161, 1983.
- Carmeliet, E., and K. Mubagwa. "Changes by Acetylcholine of Membrane Currents in Rabbit Cardiac Purkinje Fibres." *J. Physiol.*, vol. 371, pp. 201-217, 1986.
- Cordeiro, J. M., K. W. Spitzer, and W. R. Giles. "Repolarizing K<sup>+</sup> Currents in Rabbit Heart Purkinje Cells." *J. Physiology*, vol. 508.3, pp. 811-823, 1998.
- Demir, S. S., J. W. Clark, and W. R. Giles. "Parasympathetic Modulation of Sinoatrial Node Pacemaker Activity in Rabbit Heart: a Unifying Model." *Amer. J. Physiol.*, vol. 276, pp. H2221-H2244, 1999.
- Demir, S. S., J. W. Clark, C. R. Murphey, and W. R. Giles. "A Mathematical Model of a Rabbit Sinoatrial Node Cell." *Amer. J. Physiol.*, vol. 266, pp. C832-C852, 1994.
- Dexter, F., M. N. Levy, and Y. Rudy. "Mathematical Model of the Changes in Heart Rate Elicited by Vagal Stimulation." *Circ. Res.*, vol. 65, pp. 1330-1339, 1989a.
- Dexter, F., Y. Rudy, and G. M. Saidel. "Mathematical Model of Acetylcholine Kinetics in Neuroeffector Junctions." *Am. J. Physiol.*, vol. 266 (*Heart Circ. Physiol.*, vol. 35), pp. H298-H309, 1994.
- Dexter, F., G. M. Saidel, M. N. Levy, and Y. Rudy. "Mathematical Model of Dependence of Heart Rate on Tissue Concentration of Acetylcholine." *Am. J. Physiol.*, vol. 256 (*Heart Circ. Physiol.*, vol. 25), pp. H520-H526, 1989b.

- DiFrancesco, D. "Regulation of the Pacemaker Current by Acetylcholine." *Vagal Control of the Heart: Experimental Basis and Clinical Implications*, M. N. Levy and P. J. Schwartz (editors), Armonk, NY: Futura Publishing Co., 1994.
- Dokos, S., B. G. Celler, and N. H. Lovell. "Modification of DiFrancesco-Noble Equations to Simulate the Effects of Vagal Stimulation on In-Vivo Mammalian Sinoatrial Node Electrical Activity." *Ann. Biomed. Eng.*, vol. 21, pp. 321–335, 1993.
- Dokos, S., B. G. Celler, and N. H. Lovell. "Vagal Control of Sinoatrial Rhythm: a Mathematical Model." *J. Theor. Biol.*, vol. 182, pp. 21–44, 1996.
- Dokos, S., B. G. Celler, and N. H. Lovell. "Simulations of Postvagal Tachycardia at the Single Cell Pacemaker Level: A New Hypothesis." *Ann. Biomed. Eng.*, vol. 25, pp. 769–782, 1997.
- Dokos, S., N. H. Lovell, and B. G. Celler. "Review of Ionic Models of Vagal-Cardiac Pacemaker Control." *J. Theor. Biol.*, vol. 192, pp. 265–274, 1998.
- Egan, T. M., and S. J. Noble. "Acetylcholine and the Mammalian 'Slow-Inward' Current: a Computer Investigation." *Proc. Roy. Soc. Lond. I*, vol. 230, pp. 315–337, 1987.
- Feldman, R. S., J. S. Meyer, and L. F. Quenzer. Cited at <http://www.cc.emory.edu/CHEMISTRY/justice/chem190j/ache.htm>, 2000.
- Golomb, B. A. "A Review of Scientific Literature as It Pertains to Gulf War Illnesses." RAND Corporation, [http://www.gulflink.osd.mil/library/randrep/pb\\_paper/index.html](http://www.gulflink.osd.mil/library/randrep/pb_paper/index.html), 1999.
- Green, A. L. "The Kinetic Basis of Organophosphate Poisoning and Its Treatment." *Biochemical Pharmacology*, vol. 1, pp. 115–128, 1958.
- Hartzell, H. C. "Regulation of Cardiac Ion Channels by Catecholamines, Acetylcholine and Second Messenger Systems." *Prog. Biophys. Molec. Biol.*, vol. 52, pp. 165–247, 1988.
- Hassler, C. R., R. R. Moutvic, D. B. Stacey, and M. P. Hagerty. "Studies of the Action of Chemical Agents on the Heart." USAMRDC, AD-A209 219, Fort Detrick, MD, 1988.
- Hille, B. *Ionic Channels of Excitable Membranes. Second ed.*, Sunderland, MA: Sinauer Associates, 1992.
- Kale, S. S., W. R. Vieth, and K. Nho. "The Role of G-Proteins in the Regulation of Pacemaking Activity." *Ann. Biomed. Eng.*, vol. 27, pp. 746–757, 1999.
- Katz, A. M. *Physiology of the Heart. Second ed.* NY: Raven Press, 1992.

Katz, B. *The Release of Neural Transmitter Substances*. Liverpool University Press, 1969.

Koelle, G. B. (editor). *Cholinesterases and Anticholinesterase Agents*. Berlin: Springer Verlag, 1963.

Magleby, K. L., and C. F. Stevens. "A Quantitative Description of End-Plate Currents." *J. Physiol.*, vol. 223, pp. 173-197, 1972.

Maxwell, D. M., R. H. Thomsen, and S. I. Baskin. "Species Differences in the Negative Inotropic Effect of Acetylcholine and Soman in Rat, Guinea Pig, and Rabbit Hearts." *Comp. Biochem. Physiol.*, vol. 100C, pp. 591-595, 1991.

Maxwell, D. M., C. P. Vlahacos, and D. E. Lenz. "A Pharmacodynamic Model for Soman in the Rat." *Toxicology Letters*, vol. 43, pp. 175-188, 1988.

McKenzie, J. E., D. M. Scandling, N. W. Ahle, H. J. Bryant, R. R. Kyle, and P. H. Albrecht. "Effects of Soman (Pinacolyl Methylphosphonofluoridate) on Coronary Blood Flow and Cardiac Function in Swine." *Fund. Applied Toxicology*, vol. 29, pp. 140-146, 1996.

Michaels, D. C., E. P. Matyas, and J. Jalife. "A Mathematical Model of the Effects of Acetylcholine Pulses on Sinoatrial Pacemaker Activity." *Circ. Res.*, vol. 55, pp. 89-101, 1984.

Michelson, M. J., and E. V. Zeimal. *Acetylcholine*. Oxford: Pergamon Press, 1973.

Noble, D., and S. J. Noble. "A Model of Sinoatrial Node Electrical Activity Based on a Modification of the DiFrancesco-Noble (1984) Equations." *Proc. Roy. Soc. Lond. B*, vol. 230, pp. 295-304, 1984.

Noble, D., S. J. Noble, G. C. L. Bett, et al. "The Role of Sodium-Calcium Exchange During Cardiac Action Potential." *Ann. NY Acad. Sci.*, vol. 639, p. 334, 1991.

Osterrieder, W., A. Noma, and W. Trautwein. "On the Kinetics of the Potassium Channel Activated by Acetylcholine in the S-A Node of the Rabbit Heart." *Pfluegers Arch.*, vol. 386, pp. 101-109, 1980.

Osterrieder, W., Q. F. Yang, and W. Trautwein. "The Time Course of the Muscarinic Response to Iontophoretic Acetylcholine Application to the Rabbit Heart." *Pfluegers Arch.*, vol. 389, pp. 283-291, 1981.

Oxsoft Ltd. *Oxsoft Heart Program Manual, ver. 4.4*. Oxford, England, 1997.

Purves, R. D. "The Time Course of Cellular Responses to Iontophoretically Applied Drugs." *J. Theor. Biol.*, vol. 65, pp. 327-344, 1977.

- Rosenberry, T. L. "Quantitative Simulation of Endplate Currents at Neuromuscular Junctions Based on the Reaction of Acetylcholine With Acetylcholine Receptor and Acetylcholinesterase." *Biophys. J.*, vol. 26, pp. 263–289, 1979.
- Roth, A., I. Zellinger, M. Arad, and J. Atsmon. "Organophosphates and the Heart." *Chest*, vol. 103, pp. 576–582, 1993.
- Sears, C. E., P. Noble, D. Noble, and D. J. Paterson. "Vagal Control of Heart Rate Is Modulated by Extracellular Potassium." *J. Autonomic Nervous System*, vol. 77, pp. 164–171, 1999.
- Sidell, F. R., E. T. Takafuji, and D. R. Franz. *Medical Aspects of Chemical and Biological Warfare*. Office of the Surgeon General at TMM Publications, Borden Institute, Walter Reed Army Medical Center, Washington, DC, 1997.
- Sweeney, R. E., and D. M. Maxwell. "A Theoretical Model of the Competition Between Hydrolase and Carboxylesterase in Protection Against Organophosphorus Poisoning." *Math. Biosciences*, vol. 160, pp. 175–190, 1999.
- Trautwein, W., and J. Dudel. "Zum Mechanismus der Membranwirkung des Acetylcholin an der Herzmuskelfaser." *Pfluegers Archiv.*, vol. 266, pp. 324–334, 1958.
- Wang, Y. G., J. Hueser, L. A. Blatter, and S. L. Lipsius. "Withdrawal of Acetylcholine Elicits  $Ca^{++}$  Induced Delayed Afterpolarizations in Cat Atrial Myocytes." *Circulation*, vol. 96, pp. 1275–1281, 1997.
- Yanagihara, K., A. Noma, and H. Irisawa. "Reconstruction of Sinoatrial Node Pacemaker Potential Based on the Voltage Clamp Experiments." *Jap. J. Physiology*, vol. 30, pp. 841–857, 1980.
- Zang, W. J., X. J. Yu, H. Honjo, M. S. Kirby, and M. R. Boyett. "On the Role of G Protein Activation and Phosphorylation in Desensitization to Acetylcholine in Guinea-Pig Atrial Cells." *J. Physiology*, vol. 464, pp. 649–679, 1993.
- Zhang, H., A. V. Holden, D. Noble, and M. R. Boyett. "Modeling the Chronotropic Effects of Acetylcholine on the Pacemaker Activity of the Rabbit Sinoatrial Node." *J. Physiology*, vol. 521P, p. 24P, 1999.

## **Appendix**

INTENTIONALLY LEFT BLANK.

## Membrane Ionic Model

Yanagihara et al.,<sup>1</sup> using the Hodgkin-Huxley formalism for the rabbit SA node, used the following membrane current models.

### (1) Slow Inward Current

$$i_s = (0.95d + 0.05)(0.95f + 0.05)\bar{i}_s \quad (\text{A-1})$$

$$\alpha_d = \frac{1.045 \times 10^{-2}(E + 35)}{1 - \exp(-(E + 35)/2.5)} + \frac{3.125 \times 10^{-2}E}{1 - \exp(-E/4.8)} \quad (\text{A-2})$$

$$\beta_d = \frac{4.21 \times 10^{-3}(E - 5)}{\exp((E - 5)/2.5) - 1} \quad (\text{A-3})$$

$$\alpha_f = \frac{3.55 \times 10^{-3}(E + 20)}{\exp((E + 20)/5.633) - 1} \quad (\text{A-4})$$

$$\beta_f = \frac{9.44 \times 10^{-4}|E + 60|}{1 + \exp(-(E + 29.5)/4.16)} \quad (\text{A-5})$$

$$\bar{i}_s = 12.5(\exp(E - 30)/15) - 1 \quad (\text{A-6})$$

<sup>1</sup> Yanagihara, K., A. Noma, and H. Irisawa. "Reconstruction of Sinoatrial Node Pacemaker Potential Based on the Voltage Clamp Experiments." *Jap. J. Physiology*, vol. 30, pp. 841-857, 1980.

(2) Fast Sodium Current

$$i_{Na} = m^3 \bar{h} \bar{i}_{Na} \quad (A-7)$$

$$\alpha_m = \frac{E + 37}{1 - \exp(-(E + 37)/10)} \quad (A-8)$$

$$\beta_m = 40 \exp(-5.6 \times 10^{-2} (E + 62)) \quad (A-9)$$

$$\alpha_h = 1.209 \times 10^{-3} \exp(-(E + 20)/6.534) \quad (A-10)$$

$$\beta_h = \frac{1}{\exp(-(E + 30)/10) + 1} \quad (A-11)$$

$$\bar{i}_{Na} = 0.5(E - 3) \quad (A-12)$$

(3) Hyperpolarization-Activated Current

$$i_h = q \bar{i}_h \quad (A-13)$$

$$\alpha_q = \frac{3.4 \times 10^{-4} (E + 100)}{\exp((E + 100)/4.4) - 1} + 4.95 \times 10^{-5} \quad (A-14)$$

$$\beta_q = \frac{5 \times 10^{-4} (E + 40)}{1 - \exp(-(E + 40)/6)} + 8.45 \times 10^{-5} \quad (A-15)$$

$$\bar{i}_h = 0.4(E + 25) \quad (A-16)$$

(4) Potassium Current

$$i_k = p\bar{i}_k \quad (\text{A-17})$$

$$\alpha_p = \frac{9 \times 10^{-3}}{1 + \exp(-(E + 3.8)/9.71)} + 6 \times 10^{-4} \quad (\text{A-18})$$

$$\beta_p = \frac{2.25 \times 10^{-4}(E + 40)}{\exp((E + 40)/13.3) - 1} \quad (\text{A-19})$$

$$\bar{i}_k = \frac{0.7(\exp(0.0277)(E + 90)) - 1}{\exp(0.0277(E + 40))} \quad (\text{A-20})$$

(5) Leak Current

$$i_l = 0.8(1 - \exp(-(E + 60)/20)) \quad (\text{A-21})$$

(6) Acetylcholine-Activated Potassium Current

$$i_{k,ACh} = u\bar{i}_{k,ACh} \quad (\text{A-22})$$

$$\alpha_u = \frac{12.32 \times 10^{-3}}{1 + (4.2 \times 10^{-4}/[ACh])}, \quad (\text{A-23})$$

where [ACh] = acetylcholine concentration

$$\beta_u = 0.01 \exp(0.0133(E + 40)) \quad (\text{A-24})$$

$$\bar{i}_{k,ACh} = 0.27(E + 90) \quad (\text{A-25})$$

The membrane potential,  $V_m$ , under isopotential conditions is given by

$$\frac{dV_m}{dt} = -\frac{1}{C_m} \sum_{j=1}^m i_j, \quad (\text{A-26})$$

where  $C_m$  is the membrane capacitance, and  $i_j$  s are the individual membrane currents.

### Enzyme Kinetics Formalism

Michaelis-Menten kinetics was used for the interaction of OP with AChE, i.e.,



where

- E = enzyme, AChE,
- S = substrate (i.e., reactant, here OP),
- ES = enzyme-substrate complex, and
- P = product.

Here,  $k_i$ 's are the elementary rate constants. Using the mass-action law, the concentration of each of the four species changes according to the following equations.

$$d[E]/dt = -k_1 * [E] * [S] + k_2 * [ES] + k_3 * [ES] \quad (\text{A-28})$$

$$d[S]/dt = -k_1 * [E] * [S] + k_2 * [ES] \quad (\text{A-29})$$

$$d[ES]/dt = k_1 * [E] * [S] - k_2 * [ES] - k_3 * [ES] \quad (\text{A-30})$$

$$d[P]/dt = k_3 * [ES] \quad (A-31)$$

Initial conditions and rate constants need to be appended to solve the equations. Michaelis-Menten kinetics allows simplification in that only two parameters, which represent enzyme properties, need to be specified. These are  $K_m$  and  $V_m$  defined as follows:

$$K_m = \frac{(k_2 + k_3)}{k_1} \quad (A-32)$$
$$V_m = k_3.$$

The  $K_m$  of the enzyme is the concentration of the substrate at which the rate of generation of the product is half maximal.  $V_m$  is "maximum velocity of the enzyme" (i.e., the rate of formation of the product when there is a saturating amount of substrate present). All the enzyme is complexed with the substrate so  $V_m$  is equal to  $k_3$ .

**Table A-1. Rate Constants and Concentrations Used in the Simulation**

	Symbol	Estimate	Reference
Reduction Rate	$k_1$	$2 \times 10^7 \text{ M}^{-1} \text{ s}^{-1}$	Rosenberry <sup>a</sup>
Reverse Reduction Rate	$k_2$	$5 \times 10^2 \text{ s}^{-1}$	Rosenberry <sup>a</sup>
Hydrolysis Rate	$k_3$	$1.5 \times 10^4 \text{ s}^{-1}$ $1.62 \times 10^{-3} \text{ ms}^{-1}$	Rosenberry <sup>a</sup> Bristow and Clark <sup>b</sup>
Initial ACh Concentration	$[\text{ACh}]_0$	$6 \times 10^{-8} \text{ M}$ $1 \times 10^{-6} \text{ to } 0.5 \times 10^{-7} \text{ M}$	Dexter et al. <sup>c</sup> Rosenberry <sup>a</sup> Michaels et al. <sup>d</sup>
ACh Diffusion Constant	$D$	$1 \times 10^{-5} \text{ cm}^2/\text{s}$ $9.15 \times 10^{-12} \text{ cm}^2/\text{ms}$	Rosenberry <sup>a</sup> Bristow and Clark <sup>b</sup>
Michaelis-Menten Constant	$K_m$	$0.14 \times 10^{-3}$ $0.012 \text{ ms}^{-1}$	Demir et al. <sup>e</sup> Bristow and Clark <sup>b</sup>

<sup>a</sup>Rosenberry, T. L. "Quantitative Simulation of Endplate Currents at Neuromuscular Junctions Based on the Reaction of Acetylcholine With Acetylcholine Receptor and Acetylcholinesterase." *Biophys. J.*, vol. 26, pp. 263–289.

<sup>b</sup>Bristow, D. C., and J. W. Clark. "A Mathematical Model of the Vagally Driven Primary Pacemaker." *Am. J. Physiol.*, vol. 244 (*Heart Circ. Physiol.*, vol. 13) pp. H150–H161, 1983.

<sup>c</sup>Dexter, F., G. M. Saidel, M. N. Levy, and Y. Rudy. "Mathematical Model of Dependence of Heart Rate on Tissue Concentration of Acetylcholine." *Am. J. Physiol.*, vol. 256 (*Heart Circ. Physiol.*, vol. 25), pp. H520–H526, 1989b.

<sup>d</sup>Michaels, D. C., E. P. Matyas, and J. Jalife. "A Mathematical Model of the Effects of Acetylcholine Pulses on Sinoatrial Pacemaker Activity." *Circ. Res.*, vol. 55, pp. 89–101, 1984.

<sup>e</sup>Demir, S. S., J. W. Clark, and W. R. Giles. "Parasympathetic Modulation of Sinoatrial Node Pacemaker Activity in Rabbit Heart: a Unifying Model." *Amer. J. Physiol.*, vol. 276, pp. H2221–H2244, 1999.

## Glossary

ACh	acetylcholine
AChE	acetylcholinesterase
B	constant
cAMP	cyclic AMP
$C_m$	membrane capacitance
D	diffusion coefficient of ACh
E	potential also enzyme
$i_{Ca,L}$	L-type calcium current
$i_{Ca,T}$	T-type calcium current
$i_f$	hyperpolarization-activated current
$i_K$	delayed rectifying potassium current
$i_l$	leak current
$i_{Na}$	sodium current
$i_{K,ACh}$	ACh $K^+$ current
$g_{K,ACh}$	conductance of $i_{K,ACh}$ channel
$k_i$	first-order rate constant for hydrolysis of ACh
$K_m$	Michaelis-Menten constant
M	amount of ACh release
OP	organophosphate
P	product
S	substrate

t time  
u gating variable  
V membrane potential  
x average distance between ACh release sites

Greek letters:

$\alpha$  gating coefficient of opening  
 $\beta$  gating coefficient of closing

NO. OF COPIES	<u>ORGANIZATION</u>
2	DEFENSE TECHNICAL INFORMATION CENTER DTIC DDA 8725 JOHN J KINGMAN RD STE 0944 FT BELVOIR VA 22060-6218
1	HQDA DAMO FDT 400 ARMY PENTAGON WASHINGTON DC 20310-0460
1	OSD OUSD(A&T)/ODDDR&E(R) R J TREW THE PENTAGON WASHINGTON DC 20301-7100
1	DPTY CG FOR RDA US ARMY MATERIEL CMD AMCRDA 5001 EISENHOWER AVE ALEXANDRIA VA 22333-0001
1	INST FOR ADVNCD TCHNLGY THE UNIV OF TEXAS AT AUSTIN PO BOX 202797 AUSTIN TX 78720-2797
1	DARPA B KASPAR 3701 N FAIRFAX DR ARLINGTON VA 22203-1714
1	NAVAL SURFACE WARFARE CTR CODE B07 J PENNELLA 17320 DAHLGREN RD BLDG 1470 RM 1101 DAHLGREN VA 22448-5100
1	US MILITARY ACADEMY MATH SCI CTR OF EXCELLENCE MADN MATH MAJ HUBER THAYER HALL WEST POINT NY 10996-1786

NO. OF COPIES	<u>ORGANIZATION</u>
1	DIRECTOR US ARMY RESEARCH LAB AMSRL D D R SMITH 2800 POWDER MILL RD ADELPHI MD 20783-1197
1	DIRECTOR US ARMY RESEARCH LAB AMSRL DD 2800 POWDER MILL RD ADELPHI MD 20783-1197
1	DIRECTOR US ARMY RESEARCH LAB AMSRL CI AI R (RECORDS MGMT) 2800 POWDER MILL RD ADELPHI MD 20783-1145
3	DIRECTOR US ARMY RESEARCH LAB AMSRL CI LL 2800 POWDER MILL RD ADELPHI MD 20783-1145
1	DIRECTOR US ARMY RESEARCH LAB AMSRL CI AP 2800 POWDER MILL RD ADELPHI MD 20783-1197
	<u>ABERDEEN PROVING GROUND</u>
4	DIR USARL AMSRL CI LP (BLDG 305)

NO. OF  
COPIES ORGANIZATION

4 CDR  
USMRICD  
MCMR UV PB  
S I BASKIN  
M ADLER  
D MAXWELL  
R SWEENEY  
3100 RICKETTS POINT RD  
APG MD 21010-5425

ABERDEEN PROVING GROUND

19 DIRECTOR  
US ARMY RESEARCH LAB  
AMSRL CI  
N RADHAKRISHNAN  
AMSRL CI CT  
A CELMINŠ  
AMSRL CS TT  
J POLK  
AMSRL CI H  
W STUREK  
C NIETUBICZ  
P SATYA NARAYANA  
M HURLEY  
AMSRL CI S  
A MARK  
AMSRL CI HA  
C ZOLTANI (4 CPS)  
D HISLEY  
D PRESSEL  
R NAMBURU  
AMSRL WM B  
A HORST  
E SCHMIDT  
AMSRL WM BC  
P PLOSTINS  
H EDGE

REPORT DOCUMENTATION PAGE			Form Approved OMB No. 0704-0188	
Public reporting burden for this collection of information is estimated to average 1 hour per response, including the time for reviewing instructions, searching existing data sources, gathering and maintaining the data needed, and completing and reviewing the collection of information. Send comments regarding this burden estimate or any other aspect of this collection of information, including suggestions for reducing this burden, to Washington Headquarters Services, Directorate for Information Operations and Reports, 1215 Jefferson Davis Highway, Suite 1204, Arlington, VA 22202-4302, and to the Office of Management and Budget, Paperwork Reduction Project(0704-0188), Washington, DC 20503.				
1. AGENCY USE ONLY (Leave blank)	2. REPORT DATE November 2000	3. REPORT TYPE AND DATES COVERED Final, January 1999–August 2000		
4. TITLE AND SUBTITLE A Computation Model of Soman-Induced Cardiac Toxicity (I): Simulation at the Cellular Level			5. FUNDING NUMBERS  2102020	
6. AUTHOR(S) Csaba K. Zoltani and Steven I. Baskin*				
7. PERFORMING ORGANIZATION NAME(S) AND ADDRESS(ES) U.S. Army Research Laboratory ATTN: AMSRL-CI-HA Aberdeen Proving Ground, MD 21005-5067			8. PERFORMING ORGANIZATION REPORT NUMBER  ARL-TR-2367	
9. SPONSORING/MONITORING AGENCY NAMES(S) AND ADDRESS(ES)			10. SPONSORING/MONITORING AGENCY REPORT NUMBER	
11. SUPPLEMENTARY NOTES *U.S. Army Medical Research Institute of Chemical Defense				
12a. DISTRIBUTION/AVAILABILITY STATEMENT Approved for public release; distribution is unlimited.			12b. DISTRIBUTION CODE	
13. ABSTRACT (Maximum 200 words)  Under a memorandum of understanding (MOU) between the Computational and Information Sciences Directorate (formerly the Corporate Information and Computing Directorate) of the U.S. Army Research Laboratory and the U.S. Army Medical Research Institute of Chemical Defense, results of a study to model the electrophysiological changes in the heart due to soman toxicity are reported. This, the first of a series of reports, presents a computational model of cardiac toxicity at the cellular level and shows the changes in electrical activity for a series of organophosphate (OP) dose concentrations expressed by changes in the acetylcholine concentration generated membrane currents. A plausibility argument is advanced for the consideration of an overlooked aspect of the problem, the effect of extracellular potassium ion accumulation, to the understanding of soman-induced electrophysiological chaos.				
14. SUBJECT TERMS soman, cardiac toxicity, computer simulation			15. NUMBER OF PAGES 48	
			16. PRICE CODE	
17. SECURITY CLASSIFICATION OF REPORT UNCLASSIFIED	18. SECURITY CLASSIFICATION OF THIS PAGE UNCLASSIFIED	19. SECURITY CLASSIFICATION OF ABSTRACT UNCLASSIFIED	20. LIMITATION OF ABSTRACT UL	

INTENTIONALLY LEFT BLANK.

## USER EVALUATION SHEET/CHANGE OF ADDRESS

This Laboratory undertakes a continuing effort to improve the quality of the reports it publishes. Your comments/answers to the items/questions below will aid us in our efforts.

1. ARL Report Number/Author ARL-TR-2367 (Zoltani) Date of Report November 2000

2. Date Report Received \_\_\_\_\_

3. Does this report satisfy a need? (Comment on purpose, related project, or other area of interest for which the report will be used.) \_\_\_\_\_  
\_\_\_\_\_  
\_\_\_\_\_

4. Specifically, how is the report being used? (Information source, design data, procedure, source of ideas, etc.) \_\_\_\_\_  
\_\_\_\_\_  
\_\_\_\_\_

5. Has the information in this report led to any quantitative savings as far as man-hours or dollars saved, operating costs avoided, or efficiencies achieved, etc? If so, please elaborate. \_\_\_\_\_  
\_\_\_\_\_  
\_\_\_\_\_

6. General Comments. What do you think should be changed to improve future reports? (Indicate changes to organization, technical content, format, etc.) \_\_\_\_\_  
\_\_\_\_\_  
\_\_\_\_\_

CURRENT  
ADDRESS

\_\_\_\_\_  
Organization

\_\_\_\_\_  
Name

\_\_\_\_\_  
E-mail Name

\_\_\_\_\_  
Street or P.O. Box No.

\_\_\_\_\_  
City, State, Zip Code

7. If indicating a Change of Address or Address Correction, please provide the Current or Correct address above and the Old or Incorrect address below.

OLD  
ADDRESS

\_\_\_\_\_  
Organization

\_\_\_\_\_  
Name

\_\_\_\_\_  
Street or P.O. Box No.

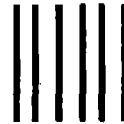
\_\_\_\_\_  
City, State, Zip Code

(Remove this sheet, fold as indicated, tape closed, and mail.)  
**(DO NOT STAPLE)**

---

**DEPARTMENT OF THE ARMY**

**OFFICIAL BUSINESS**



**BUSINESS REPLY MAIL**  
FIRST CLASS PERMIT NO 0001,APG,MD

**NO POSTAGE  
NECESSARY  
IF MAILED  
IN THE  
UNITED STATES**



**POSTAGE WILL BE PAID BY ADDRESSEE**

**DIRECTOR  
US ARMY RESEARCH LABORATORY  
ATTN AMSRL CI HA  
ABERDEEN PROVING GROUND MD 21005-5067**

---